Volume-4, Issue-6, June-2015 • ISSN No 2277 - 8160

Research Paper | Medical Science

Structural Studies and Morphology of Chemically Treated Sisal Fibre Aluminum Nitrate Composites

Asif jehan Motilal vigyan mahavidhalya Bhopal (M.P.) India

ABSTRACT

This study is essentially done to investigate the effect of chemical treatment on the structure and morphology of sisal fibre digested aluminium composites. The sisal fibre is treated with aluminum nitrate salt and mixed with constituent composite material at 1000oC temperature using annealing method. Analysis of X-ray diffraction of this treated sisal fibre revealed the crystalline nature of the composites. While the change in morphology of the product was also noticed, when treated sisal fibre was used in place of normal sisal fibre for making the composites, under Scanning Electron Microscopy. Other studies like TEM and FTIR were also done to substantiate the conclusions.

KEYWORDS : Al_2O_3, sintering & calcinations, TEM and FTIR, meta-center

Introduction

Aluminum oxides are chemical compounds composed of aluminum and oxygen. All together, there are sixteen known aluminum oxides and oxy-hydroxides [1-2]. Aluminum (III) oxide or aluminum oxide is the inorganic compound with the formula Al_2O_3. we have taken the advantage of aluminum oxide which can form hundreds of compounds with other inorganic as well as organic compounds. Thus $LiAlO_2$ has various crystalline structures such as α- $LiAlO_2$, β-$LiAlO_2$, γ-$LiAlO_2$, Layered $LiAlO_2$, Corrugated $LiAlO_2$, Goethite type $LiAlO_2$ etc. The crystalline structure of $LiAlO_2$ depends mainly on the preparation methods. Many researches prepared $LiAlO_2$ with different structures. V.R. Galakhov et al. prepared α-$LiAlO_2$ with Fm-3m space group by using solid state reaction and M. Tabuchi et al. prepared α-$LiAlO_2$ with Fm3m space group by hydrothermal synthesis [3-5]. Powder metallurgy comprises a set of processes of forming. The common denominator was the raw materials in a powder form. The reduced aluminum powder is most widely used material in the industry of powder metallurgy.

The geo-polymers were made using meta-kaolin, calcium hydroxide, sodium hydroxide, sodium silicate and water. The geo-polymers contained two or three phases, depending on whether or not calcium hydroxide was used. For geo-polymers with no calcium hydroxide, the samples contained two phases: un-reacted meta-kaolin and geo-polymer gel. To ensure geo-polymer gel was formed and to monitor the amount of the geo-polymer gel, hydrochloric acid (*HCL*) extractions were performed. For geo polymers with calcium hydroxide, samples contained three phases: unreacted meta-kaolin, geo-polymer gel and calcium silicate hydrate with aluminum substitution (CASH). In conjunction with the *HCl* extraction, salicylic acid/methanol (SAM) extractions were performed to verify the presence and amounts involved in each phase. X-ray diffraction (XRD) was used to identify crystalline phases as well as monitor the changes in the amorphous peak resulting from meta-kaolin to geo-polymer. XRD analysis showed that the geo-polymers with varying Si/Al ratios produced the same pattern. It helps us in analyzing the results. The patterns with calcium hydroxide in the geo-polymer produced an amorphous peak that was narrower and centered at higher 2θ value than the geo-polymers with no calcium hydroxide. The patterns also confirm the presence of calcium silicate hydrate in XRD patterns. Both Si and Al magic angle spinning nuclear magnetic resonance (MAS-NMR) has been used by Struble to quantitatively observe the individual silicon and aluminum structures in the different phases in the geo-polymer [6]. From Si NMR analysis, the composition and amount of the different phases in the geo-polymer could be determined. Increasing the Si/Al ratio caused a decreased strength of bonds in Si-O-Al and an increase in the strength of Si-O-Si bonds in the geo-polymer gels, which caused increase of the compressive strength in the geo-polymer. The Si NMR analysis showed that geo-polymers with calcium hydroxide produced calcium silicate hydrate that had cross-linking tetrahedral with alumina substitution in bridging tetrahedral sites [7]. The increasing amount of calcium hydroxide increased the amount of CASH and decreased the amount of the geo polymer gel. Increasing calcium hydroxide caused the Si/Al ratio of the geo-polymer gel to decrease. The combination of geo-polymer gel and CASH increased the bonding strength of the geo-polymer gel [8].

Silicon dioxide (SiO_2), is most commonly used in dielectric gates in semiconductor popularly called metal-oxide-semiconductor (MOS). These devices with Si substrate have gained importance due to their chemical and thermal stability [9]. The SiO_2 thickness is found to decrease significantly in the development of high-speed advanced semiconductor devices [10-11]. However, the gate oxide thickness cannot be reduced below 2 nm because of reliability problems associated with conventional SiO_2 and high leakage currents caused by direct tunneling across the gate dielectric film [12-13]. Based on these restrictions, high dielectric-constant materials are required as alternative gate insulators in advanced MOS devices [14-15]. Compared to SiO_2 films, high dielectric constant films can provide larger physical thicknesses and significant reductions in leakage currents for the same equivalent oxide thickness (EOT) [16-17]. Among the high dielectric constant materials, HfO_2, Al_2O_3, ZrO_2, and Ta_2O_5 have been extensively studied to solve the excessively high leakage current concern for future advanced high performance devices [18-19]. Al_2O_3 and HfO_2 are considered to be the most attractive materials among the high dielectric materials. Also, Al_2O_3 has been studied in ultra-large-scale integrated devices because it remains amorphous even after annealing at temperatures as high as 1000°C [20]. In addition, Al_2O_3 exhibits a large band gap (~ 8.8 eV), a high field strength, an excellent thermal stability, and large band offsets [21]. Our composite may be another step to explore its viability as gate in semiconductors.

Initial studies used sisal fibre as fillers in formation of composites. Hence in the present study the objective was to find effect of chemical treatment of sisal fibre and see changes (if any) on the final structure and morphology of the composite. The desired result have been obtained from the use the chemically treated sisal fibre.

Process

Aluminum Nitrate, [Al $(NO_3)_3$. $9H_2O$] and ammonium chloride (NH_4Cl) was taken in the ratio 10:4 in 500 *ml* of distilled water. The mixture was stirred till a homogenous solution is obtained. In this mixture 10 g of processed sisal fiber was added and then 1:1 solution of NH_4OH (liquid ammonia) was added to it. The mixture was left for one hour to digest. The mixture thus obtained was dried and then annealed in muffle furnace at 1000°C and kept it at that temperature for different time durations. The nomenclature of samples was: sample 1 (SP1) annealed for 15 min, sample 2 (SP2) annealed for 30 min and sample 3 (SP3) was annealed for 45 min. Table 1 below indicate some characteristics of the materials.

Table 1

Name	Symbol	Classification	A	B
Cellulose	$C_6H_{10}O_5$	C-H De-protonation	C	H
Hemicelluloses	$C_5H_{10}O_5$	C-H De-protonation	C	H
Lignin	$C_{13}H_{34}O_{11}$	C-H De-protonation	C	H

The likely chemical reaction may be as under.

$2\ Al(NO_3)_3.9\ H_2O + 3\ NH_4Cl + 3\ NH_4OH + Fiber \rightarrow Al_2O_3: fiber + 6NH_4NO_3 + 3HOCl + 18H_2O$

When aluminum nitrate reacts with ammonium chloride and ammonium hydroxide along with sisal fiber at 1000°C, aluminum oxide is formed which is confirmed through XRD analysis. The by- products like 6 NH_4NO_3, Ammonium nitrate and HOCl (hypoclorous acid) decompose at such high temperature and only aluminum oxide is left .

Result and discussion

TEM

Fig. 1(a) (b) and (c) for SP1, SP2 & SP3 respectively, shows the non linear and non uniform dispersed aluminum oxide particles of size 110.57 nm and the agglomerated fiber containing sizes of 156.92 & 284.63 nm particles of aluminum oxide. The samples appear highly strained as seen in Fig. 1 (a) (b) and (c). The presence of dislocation loops is also clearly seen. It is possible that the strain present in the sintered samples has a direct effect on the dielectric loss. The TEM micrographs show the heterogeneous micro-structured aluminum oxides. A heterogeneous distribution of the individual phases is observed in all heterogeneous systems. On the other hand, in the aluminum oxide samples particles possessed needles like morphology with non-uniform sizes in a range from 110.57 nm to 284.63 nm. These needles are less in numbers but larger in size of size ~ 30 nm. The diffraction pattern shows a higher grade of crystalline for larger quantity of aluminum oxide samples. The first Fig. 1 (a) shows the magnification 40000 which shows total palate of size of 110.57nm, the second Fig. 1 (b) shows with the magnification of 12000 which clearly shows the fibrous portion of the palate 156.92 nm and the third Fig. 1 (c) shows the magnification of 60000 which again shows the fibrous portion of the palate of size 283.62 nm.

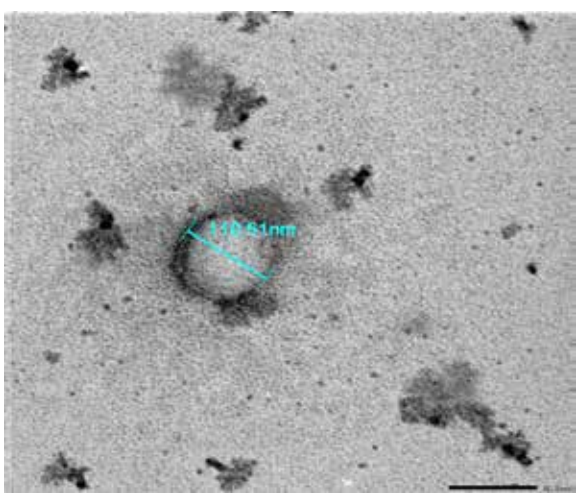

Fig.1(a)

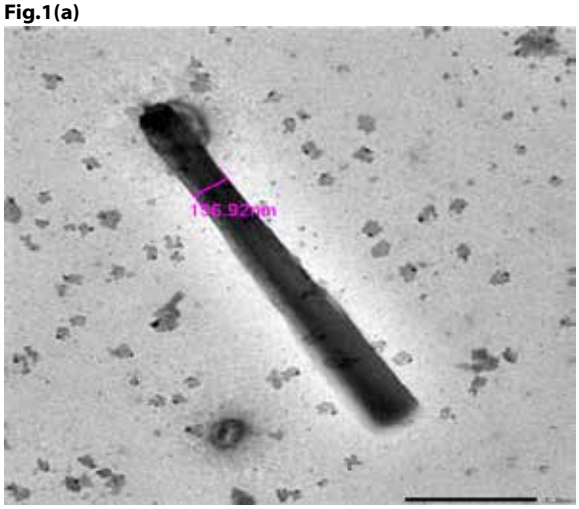

Fig.1(b)

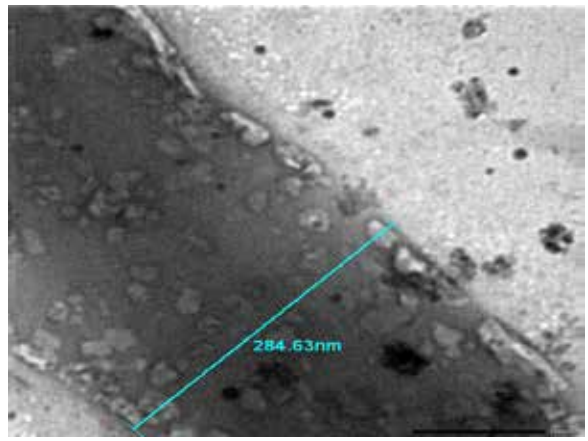

Fig. 1 (c)

Fig.1 (a) (b) and (c) TEM of Al_2O_3 to find the structure and composition of the sample prepared in our studies.

The TEM graphs show the highly homogeneous microstructure if Al_2O_3 samples the aluminum nitrate and ammonium chloride (10:4) one has still amorphous particles. The TEM investigations of the Al_2O_3 composite samples show heterogeneous distribution with needle like structure. Among the sisal fiber doped aluminum samples with the composition has a longer amount of pores in the microspores region. Hence the pores size can be adjusted by the composition according to needs of the applications TEM observations confirmed the homogeneity of the microstructure. The morphology of the composites consists of aluminum oxide needles with high aspect ratio. It is possible to synthesize materials with different porosity features and surface morphology, which result in different applications by changing the ration of individual components in oxide system [24].

FTIR

The formation of α-Al_2O_3 was supported by FTIR spectrum in figures showed that α-Al_2O_3 is known to have spinal structures which exist over a range of hydrogen content captured by the empirical formula $H_{3m}Al_{2-m}O_3$. It is clear that broad absorption bands appear at 3500-500cm^{-1} respectively, which is attributed to the stretching vibration of hydroxyl groups. The peaks at 3127.07, 1399.42 and 584.57 cm^{-1} correspond to the vibration of carboxylic acid groups. The IR transmission spectra of sisal fiber composite shown in figures from Fig. 2, 3 & 4 for SP1, SP2 & SP3 respectively, were recorded in the range 3700-3400 cm^{-1}.

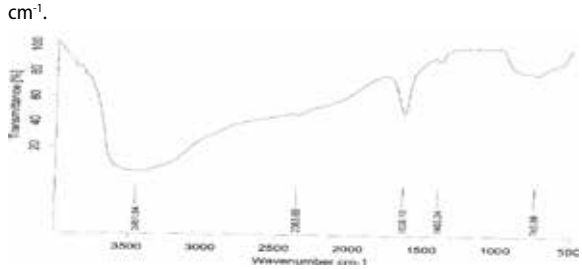

Fig. 2 Intensity of Transmittance versus wave number (courtesy SIRT-F Bhopal)

The wave numbers of Fig. 2 (SP1) 3127.0691, 2358.4974, 1641.0773, 1399.4211 and 584.5742cm^{-1} corresponded to higher transmittance in comparison to nearby wave numbers. Figure shows the widths as 1471.2957, 1716.5060, 82.7603, 40.8444 and 378.2537 cm^{-1} of IR spectra respectively.

Thus prepared samples appear homogeneous to naked eyes. The cracks or bubbles cannot be directly seen. Decrease in transmittance is associated with a shift of meta-center towards slightly higher wave number. For further increase of Al_2O_3 the intensity of this band continues to decrease. The first group of bands is also observed to decrease in transmittance [25]. The peaks at 3447.86, 1639.35 and 586.54 cm^{-1} correspond to the vibration of carboxylic acid group. The wave number of Fig. 4 (SP2) are 3447.86, 2360.13, 2072.60, 1639.35, 1397.30,

642.20 and 586.54 cm^{-1} have corresponding width of 445.6188, 60.6905, 203.3672, 82.8672, 44.0294, 92.4690 and 294.6694 cm^{-1} of IR spectra respectively.

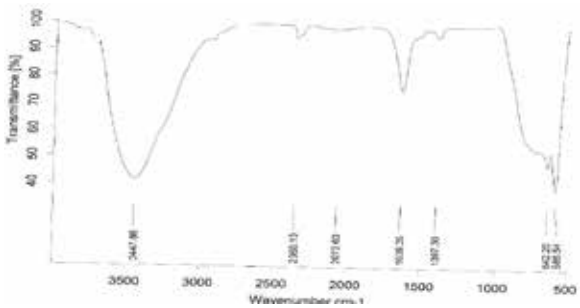

Fig. 3 Quantum of Transmittance versus wave number another sample (courtesy SIRT-F Bhopal).

The peaks at 3450.73, 1638.44 and 589.85 cm^{-1} correspond to the vibration of carboxylic acid group. The wave numbers associated with low transmittance are at 3450.73, 2360.94, 1638.44, 74004 and 589.85 cm^{-1} shows the width 558.7216, 54.5087, 79.0997, 366.1014 and 46694.4103 cm^{-1} of IR spectra respectively as can be observed in Fig. 4 (SP3). The prepared sample was free from visible non-homogeneities like cracks or bubbles. Here also the decrease in transparency is accompanied with a shifting of meta-center towards slightly higher wave number. For further increase of Al_2O_3 content the transparency of this band continues to decrease. The first group of bands is also affected the same way [25].

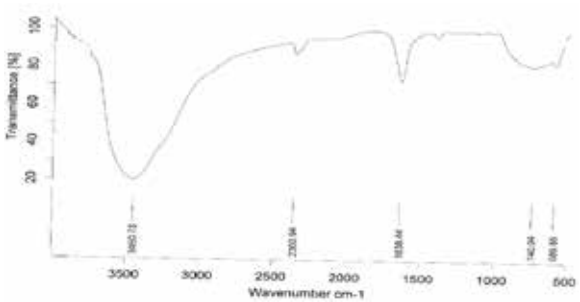

Fig.4 has several valleys imitating influence of dopants. The prominent valley at 3437 cm^{-1} is interesting (courtesy SIRT-F Bhopal).

The stronger broadening bands 3500-1000 cm^{-1} for SP1, 3400-900 cm^{-1} for SP2 and 3300-800 cm^{-1} for SP3 occurs due to the hydrogen bond between various hydroxyl groups in the product. The stronger broadening bands 3700-3400 cm^{-1} for SP1, SP2 & SP3 correspond to Al-O vibration existed under the temperature of 1000°C at 15, 30 and 45 min for SP1, SP2 and SP3 samples respectively. In agreement with other reported works. This results only from duration of annealing. We may even suggest that a series of different aluminum oxide phases is due to time of calcinations and extent of temperature (in this case 1000°C) leads to form the α-Al_2O_3 [26].

Conclusion

There is positive effect seen on properties of freshly prepared alumina composite when treated sisal fibre was taken as filler while forming the aluminium composite. Further it was noticed that mode of preparation of the composite has large influence on the final product. The effect of chemical homogeneity, fine structure, particle size and shape of the aluminum samples are found to affect the structural and chemical properties of the composites as is revealed by TEM and FTIR. The presence of moisture, cellulose, hemicelluloses, lignin and pectin also contribute to changes in composites properties. This is in agreement with results of other workers.

REFERENCES

1. Cornell, R.M, ; Schwertmann, U (2003). The aluminum oxides: structure, properties, reactions, occurrences and uses. Wiley VCH. ISBN 3-527-30274-3. | 2. Bienvenu, Y., Rodrigues, S. Manufacture of Metal Powders from Pulverulent Waste, ENSMP, Centre des matériaux, CNRS UMR 7633, France (2007). | 3. Lee, Y.S.; Sato, S.; Tabuchi, M.; Yoon, C.S.; Sun, Y.K.; Kobayakawa, K.; Sato, Y. ectrochem. Commun. 2003, 5, 549. DOI: 10.1016/S1388-2481(03)00118-8. | 4. Masaaki H.; Hiroki T.; Kei K.; Ryoji.; J. Power Sources 2011, 196, 809. DOI: 10.1016/j.jpowsour.2010.10.009. | 5. Galakhov, V.R.; Kurmaev, E.Z.; Uhlenbrock, S. Solid State Commun. 1995, 95, 347. DOI: 10.1016/0038-1098(95)00279-0. | 6. Struble, L., The effects of water on maleic and salicylic acid extraction. Cem. and Con. Res.Vol. 15. 1985. | 7. Duxson P., Provis J.L., Lukey, G. C., Separovic, F. and van Deventer J. S., J Si NMR Study of Structural Ordering Alumino-silicate Geo-polymer Gels. Langmuir 2005(21) 3028-3036. | 8. Understanding effects of silicon/aluminum ratio and calcium hydroxide on chemical composition, nanostructure and compressive strength for meta-kaolin geo-polymers by Eric Heysung Kim thesis submitted in partial fulfillment of the requirements for the degree of Master of Science in civil engineering in the graduate college of the university of Illinois at urbana-champaign, 2012. | 9. Khandelwal, A., Niimi, H., Lucovsky, G. and Henry L. H., J. Vac. Sci. Technol.\0, 1989 (2002). | 10. Packan, P. A., Science285, 2079 (1999). | 11. Schulz, M., Nature399, 729 (1999). | 12. Fukuda, H., Yasuda, M. and Iwabuchi, T., Appl. Phys.Lett.61, 693 (1992). | 13. M. Copel, M., Gribelyuk, M. A. and Gusev, E.P., Appl. Phys.Lett.76, 436 (2000). | 14. Kingon, A.I., Maria, J. P. and Streiffer, S.K., Nature406,1032 (2000). | 15. Chaneliere, C., Autran, J. L., Devine, A.B. and Balland, B., Mater. Sci. Eng. R22, 269 (1998). | 16. Wilk, G. D., Wallace, R.M. and Anthony, J. M., J. Appl.Phys.87, 484 (2000). | 17. Kim, Y., Koo, J., Han, J., Choi, S., Jeon, H. and Park, C., J. Appl. Phys.92, 5443 (2002). | 18. Gopalan, S., Onishi, K., Nieh, R., Kang, C.S., Choi, R., Cho, H.J., Krishna, S. and Lee, J. C., Appl. Phys. Lett.80, 4416 (2002). | 19. Lee, J., Koo, J., Sim, H. S. and Jeon, H., J. Korean Phys.Soc.44, 915 (2004). | 20. Chin, A., Liao, C. C., Lu, C.H., Chen W. J. and Tsai, C., Symp. VLSI Tech. Dig. 135 (1999). | 21. E. P. Gusev, M. Copel, E. Cartier, I. J. R. Baumvol, C.Krug and M. A. Gribelyuk, Appl. Phys. Lett.76, 176(2000). | 22. S yusub, Gsahaya baskaranet al Indian journal of pure &applied physics Vol. 49 May 2011. Pp 315-322. | 23. Schmittle, M.; Burghart, A. Angew. Chem. Int. Ed. Engl.1997, 36, 2550. | 24. W. Wunderlich, P. Padmaja, K.G.K. Warrier TEM characterization of sol-gel-processed alumina–silica and alumina–titania nano-hybrid oxide catalysts Journal of the European Ceramic Society 24 (2004) 313–317. | 25. S yusub, Gsahaya baskaranet al Indian journal of pure &applied physics Vol. 49 May 2011. Pp 315-322. | 26. Seyed Ali Hosseini, Aligholi Niaei, Dariush Salari Production of γ-Al2O3from Kaolin Open Journal of Physical Chemistry, 2011, 1, 23-27 doi:10.4236/ojpc.2011.12004 Published Online August 2011.